Analysis of Input Current Noise with Even Harmonics Folding Effect in a Chopper Op Amp

By **Yoshinori Kusuda**

Abstract

This article presents a theoretical analysis and measurements of the input current noise of a chopper operational amplifier that has a 10 pF input capacitance, a 5.6 nV/√Hz voltage noise PSD, and a 4 MHz unity-gain bandwidth. With a higher closed-loop gain configuration, the input current noise is dominated by the thermal noise of the dynamic conductance that occurs at the input chopper. Additionally, this theoretical analysis identifies another source of the input current noise that is caused by the amplifier's voltage noise as sampled by the dynamic conductance at the input chopper. Moreover, upon the sampling, the broadband voltage noise spectral densities are folded back to the low frequency so that the resulting current noise spectral density actually increases with wider closed-loop bandwidth, hence with smaller closed-loop gain configuration. The measured current noise is 0.28 pA/√Hz with a closed-loop gain of 10, but it increases up to 0.77 pA/√Hz with the unity-gain configuration.

I. Introduction

The chopping technique periodically corrects an amplifier's offset voltage, and therefore can achieve microvolt-level offset voltage and very little 1/f noise with its corner frequency below sub-hertz.[1,2] Hence, many chopper operational amplifiers (op amps) and instrumentation amplifiers (in-amps) have mainly been intended for sensing small input voltage that has relatively low source impedance and low signal frequency. One of its important applications is to amplify millivolt-level sensor signals representing light, temperature, magnetic field, and force, whose signal frequencies are mostly lower than kilohertz.[2] However, the switching by the input chopper introduces input bias current and input current noise that are substantially higher than those of a conventional CMOS amplifier with no chopping.[3,4] When the amplifier's input is driven by a high source impedance, this input current noise will be converted to voltage noise, which may dominate the overall amplifier's noise.[3,4]

In the article "Measurement and Analysis of Input Current Noise in Chopper Amplifiers,"[4] various possible sources of input current noise were explained, and the shot noise associated with the charge injection of the input MOS switches was identified as the dominant noise source. However, in the article "Excess Current Noise in Amplifiers with Switched Input,"[5] the thermal noise of the dynamic conductance that occurred at the input chopper was identified as the dominant noise source. In all these previous measurements, the amplifier's output voltage noise was isolated from the input chopper by feedback attenuation from the amplifier's output to input.

Although chopper op amps have been traditionally used in high closed-loop gain configurations, their low offset voltage and low 1/f noise are also demanded in low closed-loop gain and/or high source impedance configurations.[2] Therefore, it is important to understand their current noise behavior in such configurations. This brief presents input current noise analysis and measurements of a chopper op amp with both high and low closed-loop gain configurations as presented in the article "A 5.6 nV/√Hz Chopper Operational Amplifier Achieving a 0.5 µV Maximum Offset Over Rail-to-Rail Input Range with Adaptive Clock Boosting Technique."[6] It identifies another source of the input current noise that is caused by the op amp's broadband voltage noise sampled by the dynamic conductance at the input chopper. Moreover, upon the sampling, the voltage noise power spectral densities (PSDs) from even harmonic frequencies of the chopping are folded back to the low frequency, which can increase the resulting current noise PSD. Therefore, this noise source can dominate the overall input current noise when the closed-loop gain is lower so that the output voltage noise of the op amp reaches the input chopper with less attenuation.

Section II reviews previously reported input current noise sources, and then Section III explains the mechanism of the input current noise source caused by the sampled broadband voltage noise and the associated noise spectrum folding effect. Section IV conducts some numerical calculations of various current noise sources of the op amp.[6] Section V then compares the calculated current noise with simulations and measurements to validate the analysis. Section VI provides some recommendations to reduce the input current noise, and the article ends with some conclusions in Section VII.

II. Previously Reported Input Current Noise Sources

The following three current noise sources were explained in the article "Measurement and Analysis of Input Current Noise in Chopper Amplifiers." First, channel charge injections of the input switches can be approximated as an average current I_{q_ave}, leading to shot noise:

$$i_{n\_SHOT} = \sqrt{2qI_{q\_ave}} = \sqrt{4qf_{CHOP} \times (WLC_{ox})_{SW} \times (V_{GS} - V_{TH})_{SW}} \quad (1)$$

where f_{CHOP} is the chopping frequency, while $(WLC_{ox})_{SW}$ and $(V_{GS} - V_{TH})_{SW}$ are the gate oxide capacitance and the overdrive voltage of the switches, respectively.

Second, the clock drivers produce kTC noise charges sampled onto the gate oxide capacitances of the switches, and then the noise charges flow into the amplifier's inputs at every chopping:

$$i_{n\_kTC} = \sqrt{8kT\,(WLC_{ox})_{SW} \times f_{CHOP}} \quad (2)$$

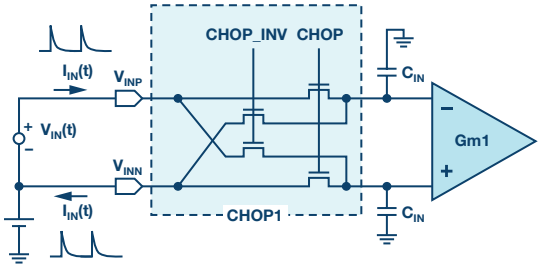

Figure 1. Dynamic input current due to chopping and input capacitances.

Third, as shown in Figure 1, a dynamic input current $I_{IN}(t)$ flows into the amplifier's input capacitors C_{IN} every time the input chopper, CHOP1, switches. When a dc voltage source $V_{IN}(t) = V_{IN\_DC}$ is applied, the averaged input currents over time I_{IN_ave} is given by:

$$I_{IN\_ave} = 2C_{IN}f_{CHOP} \times V_{IN\_DC} \quad (3)$$

The associated dynamic input conductance G_{IN_ave} and thermal noise i_{n_GIN} are then given by:

$$G_{IN\_ave} = \frac{I_{IN\_ave}}{V_{IN\_DC}} = 2C_{IN}f_{CHOP} \quad (4)$$

$$i_{n\_GIN} = \sqrt{4kTG_{IN\_ave}} = \sqrt{8kTC_{IN}f_{CHOP}} \quad (5)$$

Note that any one of the three noise equations of Equation 1, 2, and 5 consists of a unique set of the circuit and switch parameters, and therefore can dominate the overall noise depending on the values of the parameters. The shot noise shown in Equation 1 dominates the overall current noise in all three measured amplifiers[4]: an open-loop chopper in-amp and two chopper op amps with closed-loop gains of 100. This open-loop in-amp only had a 125 fF input capacitor, and thus the thermal noise of the dynamic conductance shown in Equation 5 was insignificant.

In the article "Excess Current Noise in Amplifiers with Switched Input," a chopper made of discrete FETs was measured, and the thermal noise shown in Equation 5 dominated the overall current noise when discrete capacitors ranging from 10 pF to 100 pF were added. Note that the current noise increased with the capacitor value.

III. Current Noise Caused by Sampled Voltage Noise and Noise Spectrum Folding Effect

The dynamic conductance itself generates the thermal current noise as suggested by Equation 5, but its sampling action also converts the voltage noise across the input chopper to current noise.

Dynamic Input Current Caused by Sampled AC Input Voltage

The dynamic input current with a dc input voltage is given by Equation 3. Let us now consider a case with an ac sinusoidal differential input voltage $V_{IN}(t)$ at the frequency of 2 × f_{CHOP}, as shown in Figure 2. It can be seen that $V_{IN}(t)$ reaches its peak value V_{IN_AC} when the chopping clocks CHOP and CHOP_INV switch. Consequently, this ac differential input voltage results in a dynamic input current $I_{IN}(t)$ in the same manner as a dc differential input voltage does, so that its time-averaged current I_{IN_ave} is given by:

$$I_{IN\_ave} = 2C_{IN}f_{CHOP} \times V_{IN\_AC} \quad (6)$$

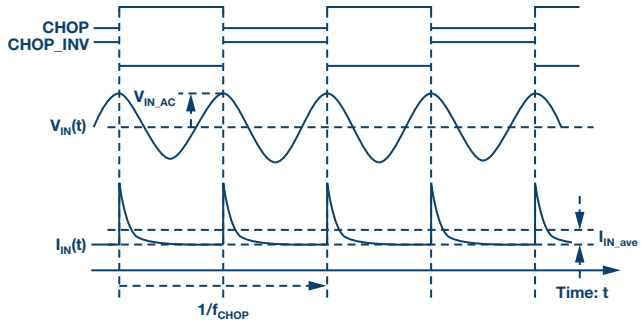

Figure 2. Dynamic input current waveform with ac differential input voltage.

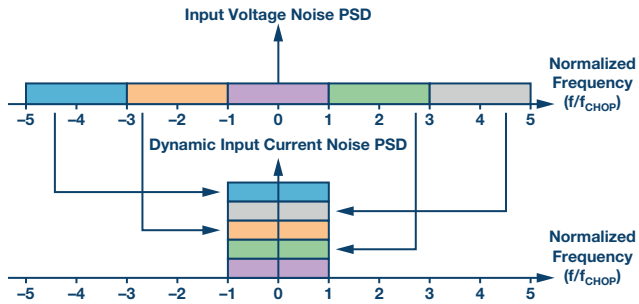

Figure 3. Noise spectrum folding effect while voltage noise PSD is sampled and converted to current noise PSD.

When the phase difference between the input voltage and the chopping clocks is random, the equation can be rewritten using the rms values of the input voltage V_{IN_RMS} and the resulting input current $I_{IN\_ave\_RMS}$:

$$I_{IN\_ave\_RMS} = 2C_{IN}f_{CHOP} \times V_{IN\_RMS} \quad (7)$$

The input current will also occur in the same manner, when an ac input differential voltage at a higher even harmonic frequency of the chopping (for example, 4 × f_{CHOP} or 6 × f_{CHOP}) is applied.

Input Current Noise PSD Caused by Sampled Voltage Noise PSD and Noise Spectrum Folding Effect

When the input voltage has frequency spectrum including multiple even harmonic frequencies of the chopping, they are all folded back to low frequency, which is known as the noise spectrum folding effect.[1] The chopping is considered a modulation technique rather than a sampling technique. However, this dynamic input current occurs based on the sampled input voltages, rather than the continuous input voltage, so that noise spectrum folding occurs. In other words, the amount of the averaged dynamic current is only determined by the differential input voltages at the instance of the chopping, rather than the differential input voltage at any other time.

Figure 3 illustrates the noise spectrum folding effect with the consideration that an input voltage noise PSD is equal to e_n from dc to 5 × f_{CHOP} but is zero above 5 × f_{CHOP}. This results in an input current noise PSD from dc to ±f_{CHOP}, the Nyquist frequency. The input voltage noise PSD $e_n(f_{en})$ between ±f_{CHOP} will contribute to the input current noise PSD $i_{n\_en\_GIN\_0}(f)$ with no frequency shift:

$$i_{n\_en\_GIN\_0}(f_{in}) = 2C_{IN}f_{CHOP} \times e_n(f_{en}) \quad (8)$$

where f_{en} and f_{in} are the frequencies of the input voltage noise PSD and the resulting input current noise PSD, respectively. The input voltage noise PSD above f_{CHOP} and below 3 × f_{CHOP} will contribute to the input current noise PSD with a frequency shift of –2 × f_{CHOP}:

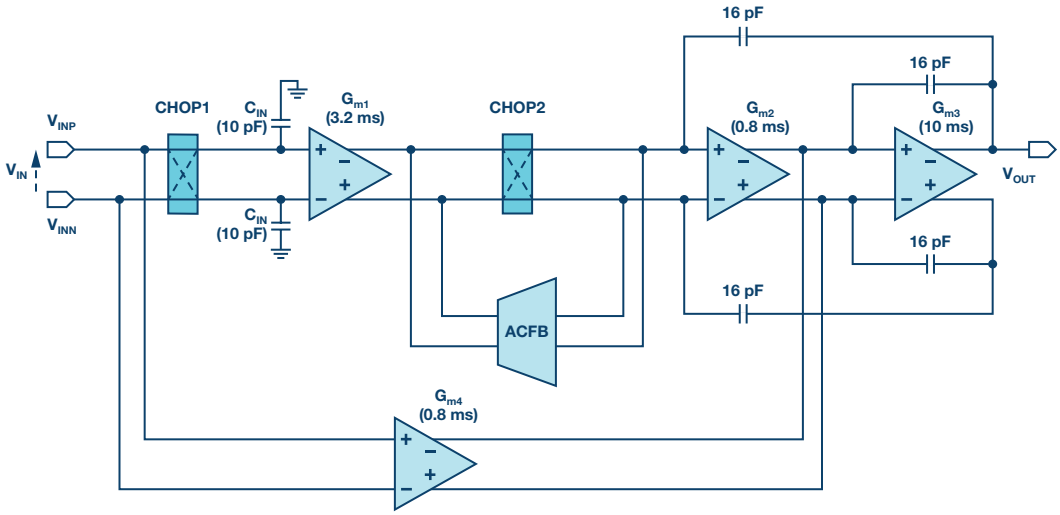

Figure 4. Chopper op amp diagram.

$$i_{n\_en\_GIN\_2fCHOP}(f_{in}) = 2C_{IN}f_{CHOP} \times e_n(f_{en} - 2f_{CHOP}) \quad (9)$$

The total input current noise PSD $i_{n\_en\_GIN\_RSS}(f)$ is obtained by summing the PSDs folded from all frequencies within the op amp's closed-loop bandwidth including those in Equation 8 and Equation 9, in the root sum square (RSS) manner:

$$i_{n\_en\_GIN\_RSS}(f_{in}) = 2C_{IN}f_{CHOP}\sqrt{\sum_{n=-\infty}^{\infty} e_n^2(f_{en} - 2nf_{CHOP})} \quad (10)$$

When the voltage noise PSD is flat at e_n and is band limited at a frequency of f_{en_BW}, the resulting low frequency current noise PSD is given by:

$$i_{n\_en\_GIN\_RSS} = 2C_{IN}f_{CHOP} \times e_n \times \sqrt{1 + \frac{f_{en\_BW}}{f_{CHOP}}} \quad (11)$$

When $f_{en\_BW}/f_{CHOP} >> 1$, the equation can be approximated to:

$$i_{n\_en\_GIN\_RSS} \cong 2C_{IN}\sqrt{f_{CHOP} \times f_{e\_BW}} \times e_n = 2C_{IN}\sqrt{f_{CHOP}} \times e_{n\_RMSINT} \quad (12)$$

where $e_n \times \sqrt{f_{en\_BW}}$ is replaced by the integrated rms voltage noise e_{n_RMSINT}. This input current noise source is approximately proportional to the rms voltage noise at the differential inputs, the input capacitor size, and the square root of the chopping frequency.

IV. Input Current Noise Estimation in a Chopper Op Amp

Chopper Op Amp Block Diagram

The chopper op amp presented in "A 5.6 nV/√Hz Chopper Operational Amplifier Achieving a 0.5 μV Maximum Offset Over Rail-to-Rail Input Range with Adaptive Clock Boosting Technique" is analyzed, simulated, and measured in this and later sections. This op amp is realized in a 0.35 μm CMOS process augmented by 5 V transistors, and it achieves a voltage noise PSD of 5.6 nV/√Hz and a unity-gain bandwidth of 4 MHz. Its block diagram is shown in Figure 4, and Table 1 summarizes the parameters of the input chopper (CHOP1). To realize rail-to-rail input common-mode range, the input transconductance amplifier stage G_{m1} consists of n-channel and p-channel differential pairs, both of which contribute to the input capacitances C_{IN}. Moreover, the larger size of the input MOS devices is needed to increase the transconductance of G_{m1} in a power efficient manner. Each of the four switches in the input chopper CHOP1 is realized by an NMOS, and its gate voltage is adaptively biased based on the input voltage, so that its overdrive voltage is constant at 0.5 V with the changes of the input voltage.

Table 1. Parameters of the Input Chopper (CHOP1)

Parameter	Explanation	Value	Unit
f_{CHOP}	Chopping frequency	200	kHz
C_{IN}	Input capacitance of G_{m1}	10	pF
R_{FB}	Gate oxide capacitance of a switch in CHOP1	30	fF
$(V_{GS}–V_{TH})_{SW}$	Gate overdrive voltage of a switch in CHOP1	0.5	V
k	Boltzmann constant	1.38×10^{-23}	J/K
T	Absolute temperature	300	K
q	Unit electron charge	1.60×10^{-19}	C

Voltage Noise Across Differential Input Terminals

To calculate the current noise PSD shown in Equation 12, the integrated rms voltage noise v_{in_RMSINT} needs to be known. The chopper op amp is simulated with closed-loop gains = 1, 2, 5, and 10. Figure 5 (a) and (b) show the voltage noise PSDs and their integrated rms noise, respectively, across the differential inputs of the op amp. All the simulations in this article are conducted by the SpectreRF periodic noise simulation (P_{NOISE}) to consider switching effects of the chopping.[7] The noise PSDs are flat below 100 kHz thanks to the chopping, but peak at the chopping frequency of 200 kHz.[6] Note that the figures present the noise at the op amp's differential inputs rather than its output, so that the noise PSDs below 100 kHz are constant with different closed-loop gains. The noise PSDs also increase above 1 MHz and are dominated by the thermal noise of G_{m2}, G_{m3}, and G_{m4} due to the gain drop of G_{m1}. Therefore, their integrated rms noise also increases above 1 MHz, especially with lower closed-loop gain, mainly due to the higher closed-loop bandwidth. The integrated rms voltage noise across the differential inputs is 11 μV rms with gain = 10, but is 68 μV rms with gain = 1.

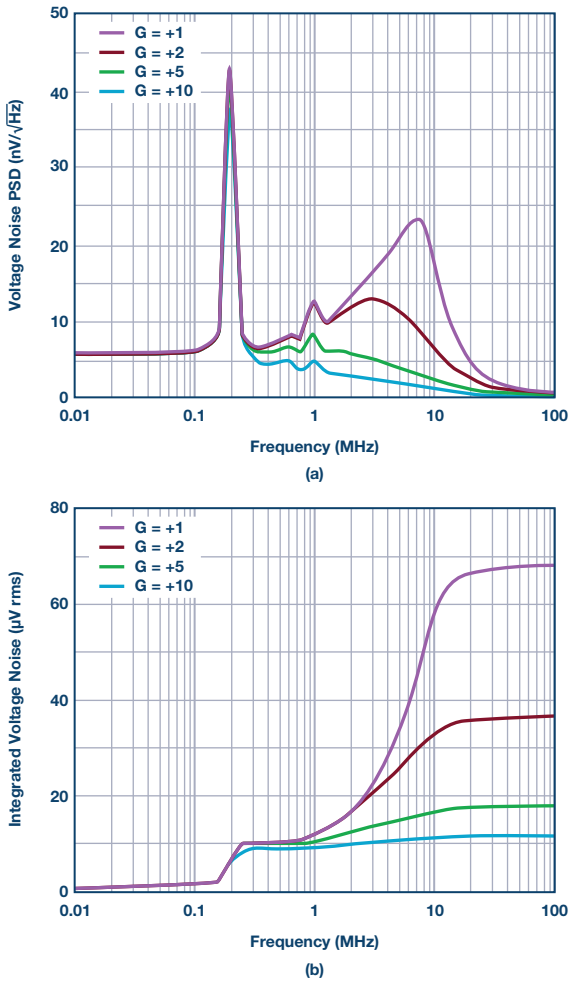

Figure 5. Simulated differential input voltage noise of the chopper op amp.

Estimation of Each Input Current Noise Source

This simulated integrated rms voltage noise is then applied to Equation 12 to calculate the current noise PSDs. Additionally, the current noise PSDs caused by the other noise sources[4] are calculated by applying the parameters in Table 1 to Equation 1, Equation 2, and Equation 5. Figure 6 shows the calculated current noise PSDs of the four noise sources with closed-loop gains from 1 to 10. The current noise PSD caused by the sampled broadband voltage noise PSD (Equation 12) dominates the total current noise PSD at closed-loop gains of 1 and 2. It decreases with higher closed-loop gains and only contributes to the total input current noise PSD by 7% at the closed-loop gain of 10. Instead, the total current noise PSD is dominated by the thermal noise of the dynamic conductance itself (Equation 5), and thus becomes nearly constant with the closed-loop gain above 5. Therefore, it is sufficient to evaluate the current noise with the closed-loop gain up to 10 for this op amp.[6]

V. Simulation and Measurement Results

To validate the analysis, the calculated total current noise PSDs shown in Figure 6 are compared with the simulation and measurement results. Both P_{NOISE} simulation and measurement are performed using a circuit setup, as shown in Figure 7. The voltage noise PSD e_{n_OUT} is measured by shorting R_S, and then the overall noise PSD $e_{n\_OUT\_RS}$ is measured with R_S = 100 kΩ. The current noise PSD i_{n_IN} is then given by:

$$i_{n\_IN} = \frac{\sqrt{\frac{(e_{n\_OUT\_RS}^2 - e_{n\_OUT}^2)}{G_{TOT}^2} - 4kTR_S}}{R_S} \quad (13)$$

$$G_{TOT} = \left(1 + \frac{R_F}{R_G}\right) \times G_{POST} \quad (14)$$

where $(1 + R_F/R_G)$ is the closed-loop gain around the op amp and G_{POST} = 100 is a post gain to ease the measurement by the dynamic signal analyzer HP 35670A. Note that in Equation 13 $e_{n\_OUT\_RS}$ and e_{n_OUT} are subtracted in RSS manner, because the current noise PSD is mostly caused by the folded noise from the higher frequencies and is thus uncorrelated with the voltage noise PSD.

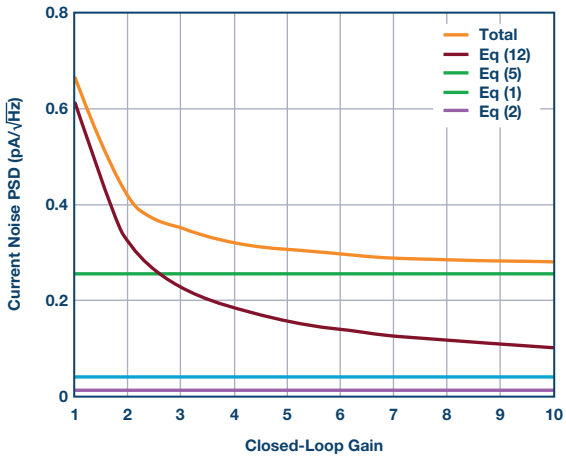

Figure 6. Calculated input current noise contribution from the different sources.

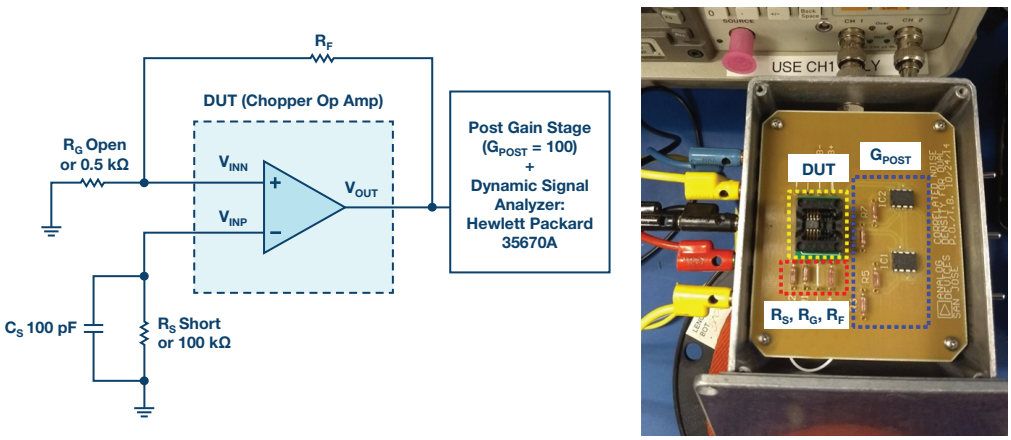

Figure 7. Circuit setup for input current noise simulations and measurements.

An external capacitor C_S = 100 pF limits the noise bandwidth of R_S at the cutoff frequency of 16 kHz. In this case, the thermal noise of R_S is sufficiently attenuated at the first even harmonic frequency of the chopping (400 kHz), and thus does not contribute to the current noise through the noise spectrum folding effect. On the other hand, the op amp's broadband output voltage noise reaches the negative input V_{INN}, sampled by the dynamic conductance at the input chopper, and can significantly contribute to the current noise. This resulting current noise PSD in the low frequency is then converted to the voltage noise again by R_S, which can be measured at the output of the post gain stage.

Figure 8 shows the simulated and measured input current noise PSDs over the frequency with gain = 1 configuration (R_G is open and R_F is short in Figure 7). At 0.01 kHz, the simulated and measured noise PSDs are 0.69 pA/√Hz and 0.78 pA/√Hz, respectively. The noise PSDs then start dropping at the 16 kHz cutoff frequency made by R_S and C_S. Figure 9 shows the input current noise PSDs at 0.01 kHz with different closed-loop gains to compare the calculated values in Figure 6 with the simulation and measurement results. Both the simulated and measured current noise PSDs increase with lower closed-loop gains, and present good correlation with the calculation. The measured input current noise PSD is 0.28 pA/√Hz with gain = 10, but increases up to 0.77 pA/√Hz with gain = 1.

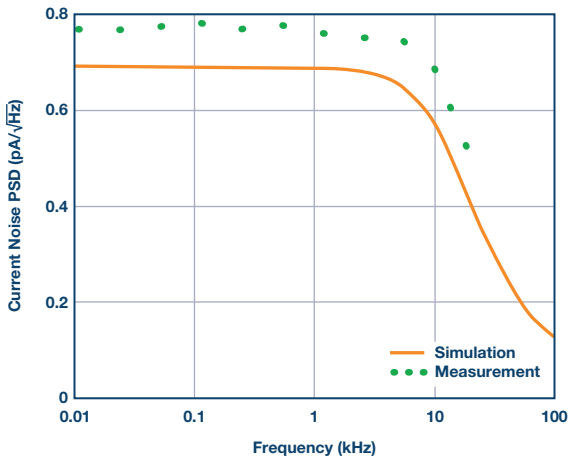

Figure 8. Input current noise PSD vs. frequency.

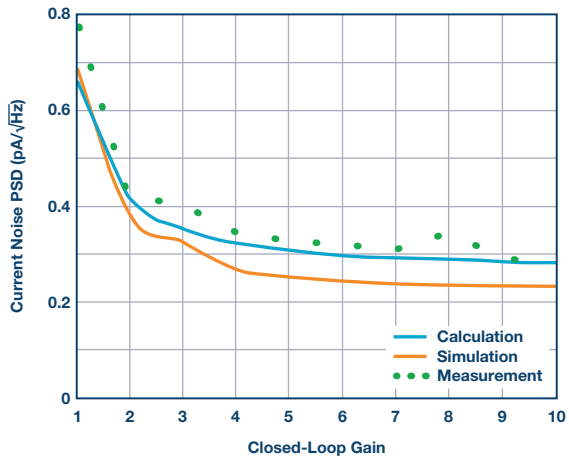

Figure 9. Input current noise PSD at 10 Hz vs. closed-loop gain.

VI. Recommendations to Reduce Input Current Noise

All the current noise sources given by Equation 1, 2, 5, and 12 increase proportionally to the square root of the chopping frequency. Additionally, the current noise sources related to the dynamic conductance at the input chopper (Equation 5 and Equation 12) increase with an amplifier's input capacitance. This implies that chopper op amps designed for lower voltage noise PSD tend to have higher input current noise PSD, since the size of their input devices needs to be increased. This trade-off must be understood to achieve optimum voltage noise and current noise PSDs with a given source impedance. When possible, complementary input pairs or input transistors under a weak inversion region should be avoided to reduce the input capacitances.

Equation 12 identifies that the current noise PSD increases with the integrated rms voltage noise across the amplifier's differential inputs, and hence with noise bandwidth. Compared to open-loop chopper in-amps, chopper op amps are more vulnerable to this noise source, since their output noise can reach their input through the feedback network. When possible, a higher closed-loop gain can be used to decrease the noise bandwidth. Another way to decrease the noise bandwidth is to place capacitor(s) in parallel with R_G, R_S, and/or across the amplifier's differential inputs as shown in Figure 7.

VII. Conclusion

This article identified another input current noise source that is caused by the amplifier's broadband voltage noise sampled by the dynamic conductance at the input chopper. It also identified that, unlike the other noise sources previously reported, this current noise PSD increases with wider closed-loop bandwidth because of the noise spectrum folding effect associated with the input chopper. This analysis was confirmed by the measurements that showed 0.28 pA/√Hz current noise with gain = 10, and 0.77 pA/√Hz current noise with gain = 1 due to the increased closed-loop bandwidth. Some recommendations were provided for amplifier designers and users to reduce input current noise of chopper amplifiers. Table 2 compares the overall performance of the chopper op amp evaluated in this article[6] with other recent chopper op amps that have similar voltage noise PSD.[8, 9, 10]

Table 2. Specifications of the Chopper Op Amp

Parameter	This Work	LMP2021	MAX44250	OPA388
Supply Current (mA)	1.4	0.95	1.17	1.7
Chopping Frequency (kHz)	200	30	60	150
Gain Bandwidth Product (MHz)	4.0	5.0	10.0	10.0
Max Offset Voltage (µV)	0.5	5.0	8.5	5.0
Max Input Bias Current (pA)	400	100	1400	350
Voltage Noise PSD (nV/√Hz)	5.6	11.0	6.2	7.0
Current Noise PSD (pA/√Hz)	0.28	0.35	0.60	0.10

References

[1] Christian Enz and Gabor C. Temes. "Circuit Techniques for Reducing the Effect of Op Amp Imperfections: Auto-Zeroing, Correlated Double Sampling, and Chopper Stabilizationv." *Proceedings of the IEEE*, vol. 84, no. 9, pp. 1320-1324, September 1996.

[2] Yoshinori Kusuda. "Reducing Switching Artifacts in Chopper Amplifiers," Ph.D. thesis. Delft University of Technology, the Netherlands, May 2018.

[3] Qinwen Fan, Johan Huijsing, and Kofi Makinwa. "Input Characteristics of a Chopped Multi-Path Current Feedback Instrumentation Amplifier." *2011 4th IEEE International Workshop on Advances in Sensors and Interfaces (IWASI)*, June 2011.

[4] Jiawei Xu, Qinwen Fan, Johan Huijsing, Chris Van Hoof, Refet Firat Yazicioglu, and Kofi Makinwa "Measurement and Analysis of Input Current Noise in Chopper Amplifiers." *IEEE Journal of Solid-Sate Circuits*, vol. 48, no. 7, pp. 1575 to 1584, July 2013.

[5] Dietmar Drung and Christian Krause. "Excess Current Noise in Amplifiers with Switched Input." *IEEE Transactions on Instrumentation and Measurement*, vol. 64, no. 6, pp. 1455 to 1459, June 2015.

[6] Yoshinori Kusuda. "A 5.6 nV/√Hz Chopper Operational Amplifier Achieving a 0.5 µV Maximum Offset Over Rail-to-Rail Input Range with Adaptive Clock Boosting Technique." *IEEE Journal of Solid-Sate Circuits*, vol. 51 no. 9, pp. 2119 to 2128, September 2016.

[7] Ken Kundert. "Simulating Switched-Capacitor Filters with SpectreRF." Designer's Guide Consulting, Inc., July 2006.

[8] LMP2021 data sheet. Texas Instruments, September 2009.

[9] MAX44250 data sheet. Maxim Integrated, October 2011.

[10] OPA388 data sheet. Texas Instruments, December 2016.

Yoshinori Kusuda [yoshinori.kusuda@analog.com] joined Analog Devices Japan Design Center in 2004 after graduating from Tokyo Institute of Technology with an M.S. degree in physical electronics. He is currently based in San Jose, California, working for ADI's Linear Products and Solutions Group. He has been working with precision CMOS analog Designs, including standalone amplifiers and application specific mixed-signal products. This work has resulted in presentations and papers at IEEE conferences and journals, as well as 10 issued U.S. patents. From 2015 through 2018, he was registered as a guest in the Electronic Instrumentation Laboratory of TU Delft and obtained his Ph.D. on the subject of reducing switching artifacts in chopper amplifiers.

Yoshinori Kusuda